PCCP

Cite this: *Phys. Chem. Chem. Phys.*, 2012, **14**, 5100–5105

www.rsc.org/pccp

PAPER

Three-dimensionally ordered macroporous silicon films made by electrodeposition from an ionic liquid

Xin Liu,[a] Yi Zhang,[a] Dengteng Ge,[a] Jiupeng Zhao,[b] Yao Li*[a] and Frank Endres*[c]

Received 14th October 2011, Accepted 28th November 2011
DOI: 10.1039/c2cp23236g

Three dimensionally ordered macroporous (3DOM) silicon films have been made *via* ordered polystyrene (PS) templates by electrodeposition from an ionic liquid (IL). For this purpose, the ionic liquid 1-butyl-1-methylpyrrolidinium bis(trifluoromethylsulfonyl)amide ($[Py_{1,4}]Tf_2N$) with $SiCl_4$ dissolved in it was used as an electrolyte and the electrodeposition of macroporous silicon could be achieved at room temperature ($\sim$20 °C). Self-assembled PS colloidal crystals with different diameters were used as templates. Scanning electron microscopy and X-ray photoelectron spectroscopy confirm the quality of the samples, and the optical transmission measurement demonstrates that the 3DOM silicon film has a bandgap in the near infrared regime. Such a material has the potential to make 3DOM silicon feasible for electrical and optical applications.

Introduction

Three-dimensionally ordered macroporous (3DOM) materials are porous solid films possessing uniform, periodical pores that are ordered in three dimensions.[1–3] Usually, they are made by creating an inverse replica of opal-structured colloidal crystal templates (CCT), which are composed of close-packed sub-micrometre monodisperse silica or polymer spheres. 3DOM silicon would be quite interesting for current micro- and opto-electronic technologies, due to its potential to enable *e.g.* low threshold lasers through control of spontaneous emission,[4] ultra-fast optical switching,[5] and low-loss optical waveguides in three dimensions.[6,7] Moreover, 3DOM silicon has considerable potential in solid catalysis,[8] solar cells[9] and photonic crystal light emitting diode (LED),[10] to mention a few.

3DOM semiconductors are quite promising materials for photonic crystals.[11] According to theory,[12] the control of photon flux and a complete photonic bandgap requires filling the CCT with high refractive index materials to achieve the highest refractive index contrast ($\geq$ 2.8).[13] One group of materials which can meet these requirements is semiconductors. Among them, silicon is one of the most important semiconductors with a high refractive index of 3.53 at 1.1 μm.

Much attention has been paid in the literature to the fabrication of 3DOM silicon, and the main challenge is the required well ordered sub-micron 3D crystal structure. Compared with two-photon phase mask lithography[14] and multibeam interference lithography,[15] the colloidal crystal template method[16–18] is as a chemical method quite attractive due to its simplicity and low cost in comparison to the mentioned physical methods.

With the colloidal crystal template technique, which is a key technique to make 3DOM semiconductor materials or photonic crystals, A. Blanco *et al.* have *e.g.* successfully fabricated silicon photonic crystals by chemical vapor deposition using Si_2H_6, and they obtained a complete PBG at 1.55 μm and at 1.3 μm.[19,20] Whereas chemical vapor deposition is a top-down approach where the particles enter the colloidal crystal structure from the vacuum side, the template-assisted electrochemical deposition is a bottom-up alternative approach where the deposition starts at the electrode surface. One might identify three advantages: first, it is a low-cost, simple and low-temperature method. Second, it can, in principle, provide an ideal filling into topologically complex structures and has no depth limitation of a periodic inter-connected structure. Third, the electrodeposits can be quite dense, smooth and maximize the effective refractive index contrast.

However, the precursors SiX_4 and $SiHX_3$ (X = Cl, Br) used for the electrodeposition of silicon will hydrolyze rapidly in the presence of water/moisture, thus silicon cannot be obtained from aqueous solvents. The electrodeposition from organic electrolytes is possible but must be performed under an inert gas atmosphere. Although there were some attempts to electrodeposit silicon from nonaqueous solvents,[21–23] the employed baths based on aprotic solvents such as propylene carbonate and tetrahydrofuran are not suitable for the electrodeposition of 3DOM silicon as the polystyrene templates are attacked or even dissolved in such baths. These problems can be overcome by ionic liquids.

Ionic liquids (ILs) are solely composed of ions and have a few advantageous properties like negligible vapor pressure,

[a] *Center for Composite Material, Harbin Institute of Technology, Harbin, China. E-mail: liyao@hit.edu.cn; Fax: +86 45186402345; Tel: +86 451 86402345*
[b] *School of Chemical Engineering and Technology, Harbin Institute of Technology, 150001, Harbin, China*
[c] *Clausthal University of Technology, Chair of Interface Processes, D-38678 Clausthal-Zellerfeld, Germany. E-mail: frank.endres@tu-clausthal.de; Fax: +49 (0)5323 72-2460; Tel: +49 (0)5323 72-3141*

high thermal stability and often significantly wide electrochemical windows.[24] Silicon can be electrodeposited from them at room temperature.[25] In a previous study we combined the CCT method with electrodeposition from an ionic liquid and could successfully obtain 3DOM germanium films.[26] The low surface tension of ionic liquids allows a complete wetting of the PS matrix and thus an ordered electrochemical growth.[27]

Electrodeposition of silicon in the PS templates is considerably more difficult than that of germanium, and silicon–germanium, as mentioned in a previous paper.[28] The conductivity of silicon is low compared to Ge, furthermore silicon deposition is performed close to the cathodic limit of the liquid. We also found that silicon electrodeposition is more sensitive to the deposition current density than that of germanium is. In comparison to germanium the deposition current of silicon is furthermore comparably low, likely due to the lower intrinsic conductivity of Si compared to Ge. A too negative deposition potential can lead to the disintegration of the PS templates. The beginning reduction of the pyrrolidinium cation seems to have a disadvantageous effect on the spheres. As will be discussed below we found that with sphere sizes of around 200 nm the template can be disintegrated during Si deposition whereas with sphere sizes above about 400 nm this problem rather does not occur. Another complication in comparison to Ge is the rapid surface oxidation of electrodeposited Si under environmental conditions, leading to SiO_2 at the surface, which complicates an optical characterization.

In the present paper we report for the first time on well ordered 3DOM silicon films made by electrodeposition from an ionic liquid using polystyrene templates.

Experimental

The ionic liquid 1-butyl-1-methylpyrrolidinium bis(trifluoromethylsulfonyl) amide ($[Py_{1,4}]Tf_2N$, 99%) was purchased from IOLITEC (Germany) and used after drying under vacuum at 100 °C for several hours, usually leading to water contents of below 2 ppm. According to the supplier the impurity level of this liquid is: Br^-, <100 ppm; Li^+, <100 ppm; methylpyrrolidine, <1000 ppm. $SiCl_4$ (99.998%) was purchased from Alfa Aesar. Monodisperse PS spheres with average diameters of 235, 455, 515 and 582 nm and a relative standard deviation of less than 5% (based on the diameter) were synthesized by using an emulsifier-free emulsion polymerization technique.[29] Indium tin oxide (ITO) covered glass supports were used as substrates for the self-assembly of the PS spheres. For this purpose the substrates were cleaned sequentially with acetone, methanol and deionized water. Subsequently, polystyrene colloidal crystals were grown by using a controlled vertical drying method. The principle has been described in ref. 27. For the vertical self-assembly process of the PS templates, the glass substrates were placed in cylindrical vessels containing PS latex with a concentration of 0.1 vol%. The vessels were then placed in an incubator at 65 °C to dry for 3–5 days. The thickness of the colloidal crystal templates can be adjusted *via* the concentration of the PS latex. In our experiments, if a 0.1 vol% PS latex is applied to vertical deposition, templates with 10 layers of PS spheres can be obtained.

The electrochemical experiments were performed in a nitrogen-filled glove box with water and oxygen contents of below 2 ppm (Vigor Glove Box from Suzhou, China). The electrochemical cell was made of Teflon and clamped over a Viton O-ring onto the ITO conductive glass substrates with the PS colloidal crystal template on top acting as a working electrode (WE). A copper wire was in contact with the ITO substrate to provide connection to the potentiostat. An Ag wire and a Pt ring were used as quasi-reference and counter electrodes, respectively. Cyclic voltammetry (CV) measurements were performed at a scan rate of 10 mV s^{-1} between −3.5 and 2 V *vs.* the quasi reference electrode at 25 °C.

After the electrochemical experiments, the deposit was removed from the glovebox and rinsed quickly with isopropanol to avoid redundant ionic liquid left on the deposit. The PS template was removed by tetrahydrofuran and the 3DOM silicon was obtained.

The morphological characterization was performed with a Hitachi S-4800 scanning electron microscope operating at 20 kV. The unavoidable exposure of the sample to air led to a certain surface oxidation and SiO_2 could be identified. Elemental and structural analyses were also achieved by energy dispersive X-ray spectroscopy EDX and an X-ray photoelectron spectroscopy (XPS) analysis of the samples with a K-Alpha XPS System from Thermo Scientific. All binding energies were referred to the C1s peak at 284.6 eV of surface adventitious carbon.

Results and discussion

Cyclic voltammetry

Fig. 1 shows an overlay of three cyclic voltammograms, namely of the pure ionic liquid $[Py_{1,4}]Tf_2N$ on ITO (red), $[Py_{1,4}]Tf_2N$ containing 0.1 mol L^{-1} $SiCl_4$ on ITO (blue) and the same electrolyte on ITO covered with the PS template (sphere diameter = 582 nm, black). The red curve reveals that the ionic liquid $[Py_{1,4}]Tf_2N$ is electrochemically stable and pure enough to allow the electrodeposition of silicon. The blue curve shows that there are two main reduction peaks of silicon, at potentials of −2.66 V and −1.92 V, respectively. The more negative peak is clearly correlated with Si deposition[23] whereas the less negative one might be due to the reduction of $SiCl_4$ to Si_xCl_{2x+2}.[30] In the black curve, which represents Si deposition in the template, the reduction peaks are slightly shifted, which is a typical result of the non-perfect stability of the quasi reference electrode. For the purpose of the present

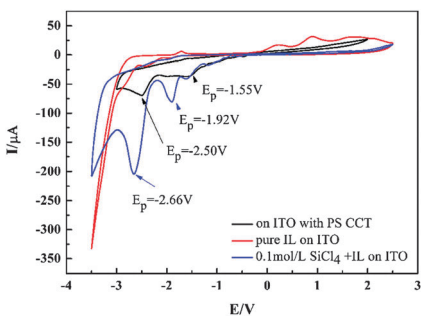

Fig. 1 Cyclic voltammograms for the electrodeposition of silicon from the ionic liquid $[Py_{1,4}]Tf_2N$; red curve: pure IL on ITO; blue curve: IL + $SiCl_4$ on ITO; black curve: IL + $SiCl_4$ on PS covered ITO (geometric surface area of the working electrode: 0.3 cm^2).

paper, where the focus is set on the electrochemical synthesis of 3DOM Si and its characterization, this slight instability is not of relevance. The most suitable deposition potential has been found to be about −2500 mV with a deposition time between 1 and 2 h. This potential represents the 2nd reduction peak in the cyclic voltammogram. More negative electrode potentials or a too long deposition time can lead to a disintegration of the template during Si growth.

XPS analysis

According to the XPS survey spectrum of 3DOM Si, the sample contains Si and some impurity elements like C, O and N due to the unavoidable exposure to air during the transfer to the XPS system and due to some residual ionic liquid adsorbed on the surface. Since the surface of electrochemically made 3DOM Si is quite reactive, the XPS spectra were also measured after a careful and controlled etching of the surface using an Ar ion beam. Fig. 2 shows how the Si 2p XPS spectra of 3DOM Si vary during Ar ion bombardment as a function of sputtering time. In curve a (before etching), there is only one peak at 103.3 eV, which is characteristic for Si–O bonds in SiO_2, indicating that the surface of the sample was completely oxidized. After 15 min of Ar^+ etching, two peaks are detected in curve b, corresponding to pure Si and SiO_2. With increasing etching time the amount of SiO_2 is reduced and the one of Si increases. After 25 min of Ar^+ etching (curve d), the peak ascribed to the SiO_2 disappears and the peak at 99.5 eV ascribed to pure Si 2p prevails. The results suggested that the deposit is initially pure silicon, which is subjected to oxidation leading to an oxide layer on the surface. Typically such an argon ion etching removes between 20 and 40 nm of SiO_2. Thus, it can be concluded that only a minor part of the 3DOM Si was oxidized to SiO_2 during the *ex situ* treatment. This surface oxidation might be reduced by a chemical surface modification in future, *e.g.* by a post-treatment with alkylchlorosilanes.

Structural characteristics

Fig. 3 shows SEM images of PS covered ITO glass supports with different sphere diameters (235, 455 and 515 nm), proving the regular structure of these templates. We investigated the influence of the PS sphere size on the microstructure of the deposits. Here, the electrodeposition experiments were carried

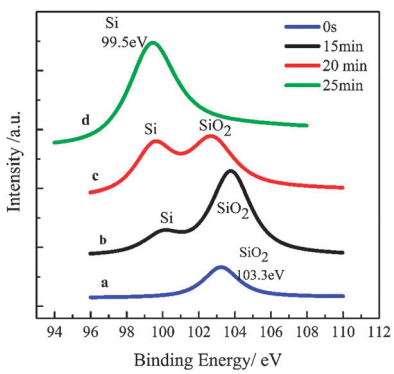

Fig. 2 Si 2p XPS spectra of 3DOM Si films electrodeposited from $[Py_{1,4}]Tf_2N$ as a function of Ar ion sputtering time.

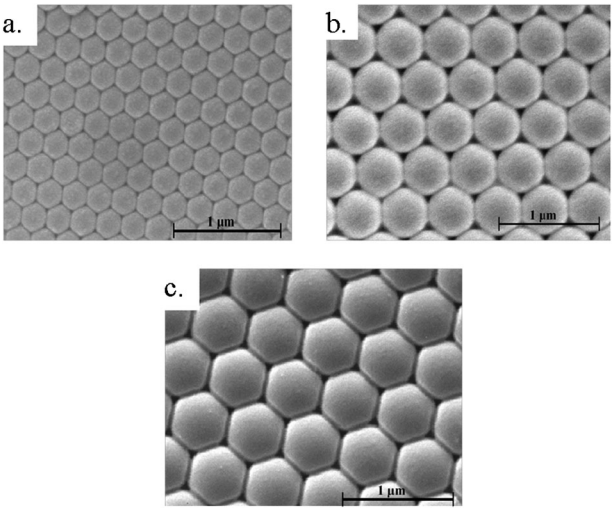

Fig. 3 SEM images of PS covered ITO glass (PS sphere diameters: (a) 235 nm, (b) 455 nm, (c) 515 nm).

out at a potential of −2.5 V *vs.* the quasi reference electrode for one hour, *i.e.* in the minimum of the 2nd reduction peak (Fig. 1, black curve). The quasi reference electrode is not perfectly stable but the shift is usually not higher than 100 mV during an experiment, thus not of importance for the deposition experiments performed here under the mentioned conditions.

A contact angle experiment of the employed ionic liquid (Fig. 4) on the ITO substrate (a) and on the PS template covered ITO surface (b) is shown in Fig. 4. On the pure ITO substrate, the contact angle of the ionic liquid is about 58° showing the wetting of the surface. The surface of the PS template has a contact angle of only 21°, which proves that the ionic liquid well wets the PS spheres. We might speculate that the reason why the contact angle is decreased on the PS covered ITO is mainly due to the roughness of these samples.

In order to obtain well ordered macroporous materials by the colloidal crystal template method from ionic liquids, two requirements have to be fulfilled. Firstly, the ionic liquid should well wet the template spheres in order to eliminate any fault in the final 3DOM structure. The higher wettability of ILs onto PS spheres leads to improved penetration of the ILs into the cavities of the PS templates. Secondly, the ionic liquid should penetrate the template array completely to allow a complete soaking of the interstices of the PS spheres and a good wetting of the electrode surface underneath the PS template.

The EDX spectrum in Fig. 5 was recorded at the point in the inset of the SEM image, showing a PS template with silicon

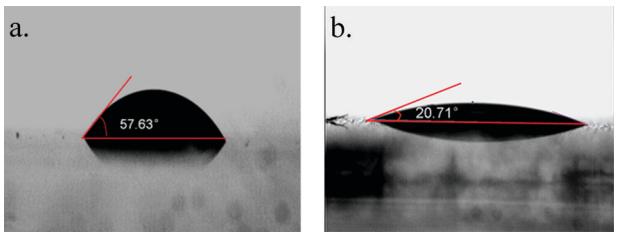

Fig. 4 Contact angle measurement of the ionic liquid on the (a) ITO substrate and (b) PS covered ITO.

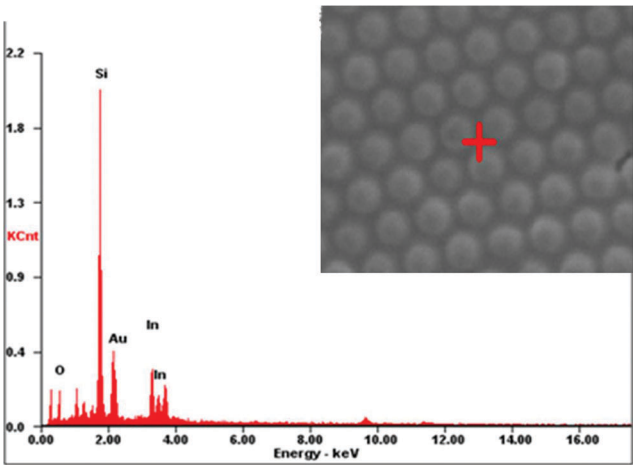

Fig. 5 EDX analysis of silicon inside the colloidal crystal templates on ITO.

deposited in the interstices. So far EDX shows Si, Au (from sputtering), In (from the substrate) and oxygen. The XPS results presented above suggest that the main part of oxygen is due to the surface oxidation of Si occurring during the transport to the SEM device.

Fig. 6 shows SEM images of 3DOM silicon films made with PS templates of different diameters, namely 235, 455 and 515 nm. The results presented in Fig. 6 reveal that the surface of the 3DOM Si films shows the periodicity given by the PS template, in principle. In Fig. 6a it is seen that the films deposited in the 235 nm PS sphere template have only a short range ordering; quite in contrast, the films seen in Fig. 6b and c rather show a longer range ordering. The regular microstructure was also assessed by a two dimensional Fast Fourier Transform (FFT) analysis of the relative SEM images (insets). The FFT's in Fig. 6b and c for the 455 nm and the 515 nm template show bright spots indicative of a long range ordering, whereas the one of the template with PS spheres of 235 nm in diameter only shows a short range ordering, in line with the SEM images.

The differences in the 3DOM structure between the three different templates are obviously associated with the different void size of the PS templates. In the PS template film with 235 nm PS spheres, the octahedral and tetrahedral voids in the template film, where the spheres are in contact with the next layer, are considerably smaller than for the other templates presented here. As the deposition of silicon in ionic liquids usually leads to silicon particles with about 50 nm diameter we might speculate that there is, in comparison with the templates having larger spheres, more space available for a regular growth. In Fig. 6, 3DOM silicon films with larger sphere diameters usually have 2–3 layers. But in Fig. 6a, for small sphere sizes, it has 4–5 layers, usually. Currently it is still difficult to get thicker films by using longer deposition time and higher electrolyte concentration, respectively, as the PS templates are then disintegrated and delaminate from the substrate in this case. This problem might be overcome at elevated temperature or with other liquids having a different interfacial behaviour.

Furthermore a hindered diffusion of $SiCl_4$ to the electrode surface and thus rather an incomplete deposition of silicon

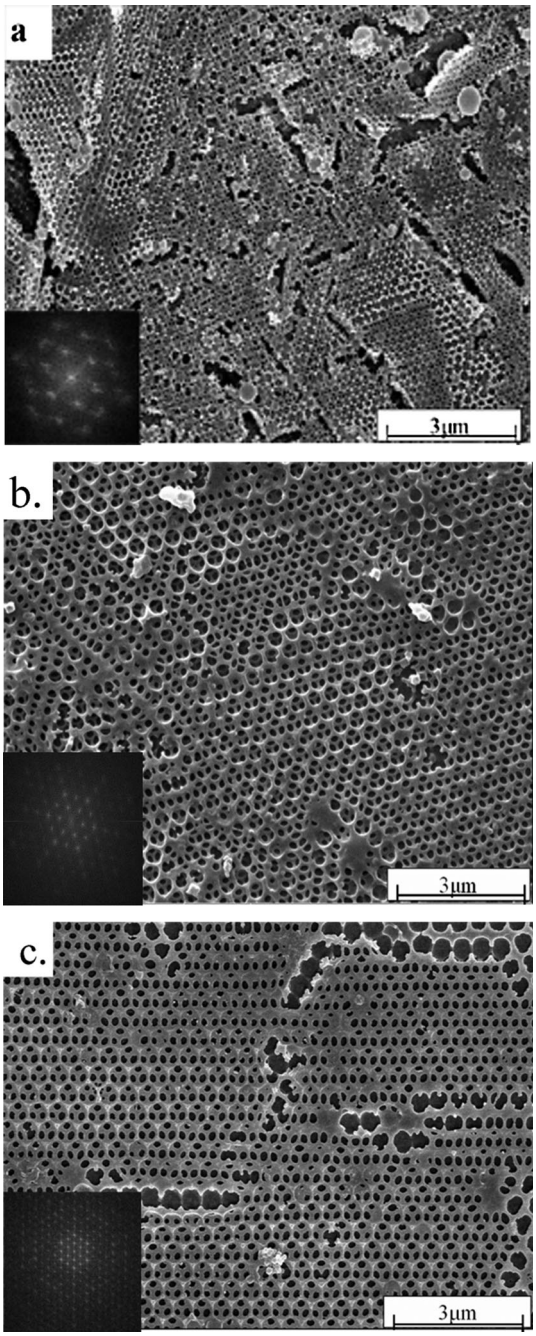

Fig. 6 SEM images of 3DOM silicon from PS templates with different diameters: (a) with 235 nm particles, (b) with 455 nm particles, (c) with 515 nm particles.

might result. Inhomogeneities in Si growth can consequently reduce the mechanical stability of the 3DOM silicon films, and the 3DOM structure might be partly destroyed collapsing during the removal of the PS templates. Based on these considerations all subsequent experiments were performed with PS templates with a larger sphere diameter.

Optical properties of 3DOM silicon film

Fig. 7 shows optical photographs of the whole 3DOM silicon film (582 nm spheres) electrodeposited for 2 h. This deposition time did not have a disadvantageous effect on the template

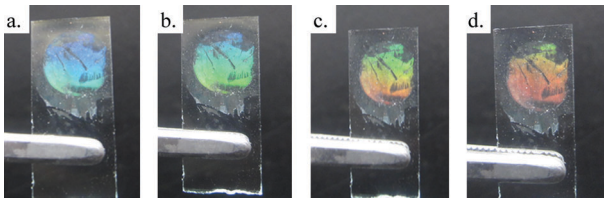

Fig. 7 Optical photographs of deposited 3DOM silicon (PS sphere size: 582 nm) on ITO showing a color change with changing the angle of incident white light.

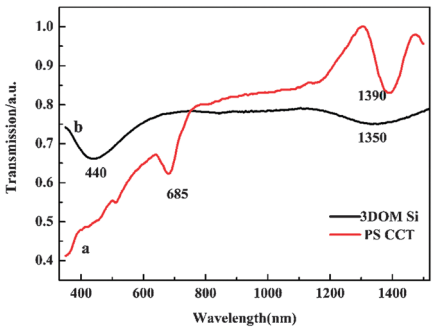

Fig. 8 Optical transmission spectra of PS colloidal crystals and of 3DOM silicon (PS/air sphere size: 582 nm).

stability. When the incident angle of the white light is slightly changed, the 3DOM silicon shows reflection colors turning to blue, green, yellow and orange. The color change of the incident angle is a result of Bragg's diffraction law and is a direct evidence for the film's behavior as a photonic crystal, modulating the incident light.

The optical transmission spectra of the PS colloidal crystal and of 3DOM silicon (PS sphere size: 582 nm) were measured, as shown in Fig. 8. The transmission spectrum of the PS colloidal crystal showed the existence of a photonic stop band centered at 1390 nm due to Bragg's diffraction (Fig. 8a). The position of the stop band is size-dependent, as concluded from a combination of Bragg's and Snell's laws,[31] $\lambda = 2d_{hkl}(n_{\mathrm{eff}}^2 - \sin^2\theta)^{1/2}$, where θ is the angle of the incident to the normal surface; n_{eff} is the effective refractive index of the structure, for PS templates, $n_{\mathrm{eff}} = \sqrt{n_{\mathrm{ps}}^2 f + n_{\mathrm{air}}^2(1-f)}$, f is the filling ratio in the FCC structure, $=74.6\%$; d_{hkl} is the distance between two diffracting (hkl) planes for the sample. For fcc opal structure photonic crystals, the most effective planes in the Bragg reflection are those with Miller indices all odd or all even.

Fig. 8b shows the transmission spectrum of 3DOM silicon. Quite a broad bandgap and a diffraction peak could be observed at around 1350 and 440 nm, respectively. The appearance of the quite broad bandgap at 1350 nm (compared with the bandgap of the PS templates) is due to several factors, including the imperfect replication of the template in the case of Si. In theory it is assumed that the 3DOM structure is defect-free which for the real sample is not the case. Furthermore, the surface oxidation of 3DOM silicon will lead to deviations from theory. The first bandgap at 1350 nm is between the bandgaps of 3DOM Si and of 3DOM SiO_2 with 582 nm pore diameter (1875 nm and 1075 nm, respectively). Based on the first bandgap, the effective refractive index of the 3DOM silicon

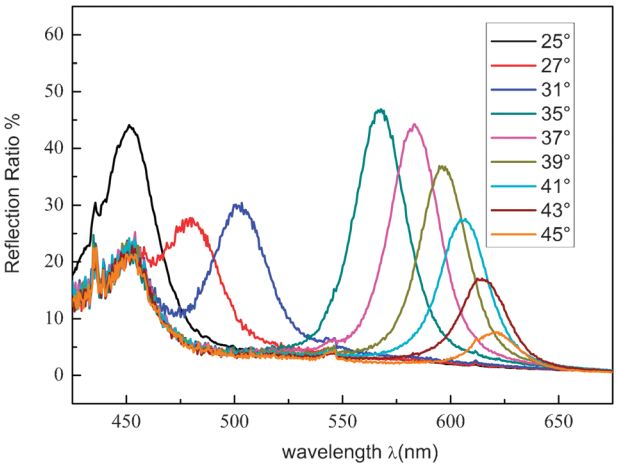

Fig. 9 Angle-resolved reflection spectra (secondary diffraction) of 3DOM silicon (sphere diameter: 582 nm).

sample n_{eff} is calculated to be 1.48, which is between those of n_{3DOMSi} and $n_{\mathrm{3DOMSiO_2}}$ (1.95 and 1.12, respectively). The results support that the surface of 3DOM silicon has indeed been oxidized, which is in agreement with the XPS results. In order to circumvent the problem of surface oxidation we will perform the optical characterization in future inside an inert gas glove box without the need to bring the sample in contact with air. Under these conditions the surface oxidation is quite slow and can be reduced further by a chemical passivation of the surface inside the glove box.

The angle resolved reflection spectra of the 3DOM silicon were obtained using an Ocean Optics fiber spectrometer, as shown in Fig. 9 and the angles in the figure represent the incidence angles from the normal, and the reflection angles probed are symmetric with the incident angle. According to the results shown in Fig. 8, it can be deduced that the angle resolved reflection in Fig. 9 originates from secondary diffraction.

Conclusions

3DOM silicon films have been made electrochemically at room temperature by a simple method, which includes self-assembled polystyrene colloidal crystals as templates and the ionic liquid $[Py_{1,4}]Tf_2N$ containing $SiCl_4$ as an electrolyte. 3DOM silicon could be made as an inverse replica of the colloid crystal template by electrodeposition of Si. The diameter of the PS spheres has a great effect on the 3DOM structure and the ones with larger diameters are more suitable for the fabrication of well ordered macroporous silicon. The photonic bandgap of 3DOM silicon was found at 1350 nm and the effective refractive index of the sample was calculated to be 1.48, which suggested that the surface of 3DOM silicon has been oxidized. The preparation of 3DOM silicon is a relatively simple way for the formation of 3DOM photonic crystals.

Acknowledgements

We thank the National Natural Science Foundation of China (No. 51010005, 90916020, 51174063), the Program for New Century Excellent Talents in University (NCET-08-0168),

the Scientific Research Foundation for the Returned Overseas Chinese Scholars of Harbin and Sino-German joint project (GZ550).

Notes and references

1 O. D. Velev, T. A. Jede, R. F. Lobo and A. M. Lenhoff, *Nature*, 1997, **389**, 447–448.
2 B. T. Holland, C. F. Blanford and A. Stein, *Science*, 1998, **281**, 538–540.
3 J. E. G. J. Wijnhoven and W. L. Vos, *Science*, 1998, **281**, 802–804.
4 M. Loncar, T. Yoshie, Y. M. Qiu, P. Gogna and A. Scherer, *Proc. Soc. Photo-Opt. Instrum. Eng.*, 2003, **5000**, 16–26.
5 T. G. Euser, H. Wei, J. Kalkman, Y. Jun, A. Polman, D. J. Norris and W. L. Vos, *J. Appl. Phys.*, 2007, **102**, 053111–053116.
6 S. A. Rinne, F. Garcia-Santamaria and P. V. Braun, *Nat. Photonics*, 2008, **2**, 52–56.
7 A. Arsenault, S. Fournier-Bidoz, B. Hatton, H. Miguez, N. Tetreault, E. Vekris, S. Wong, S. M. Yang, V. Kitaev and G. A. Ozin, *J. Mater. Chem.*, 2004, **14**, 781–794.
8 A. Lambrecht, S. Hartwig, S. L. Schweizer and R. B. Wehrspohn, *Photonic Cryst. Mater. Devices VI*, 2007, **6480**, D4800.
9 P. G. O'Brien, N. P. Kherani, A. Chutinan, G. A. Ozin, S. John and S. Zukotynski, *Adv. Mater.*, 2008, **20**, 1577–1582.
10 S. Iwamoto, Y. Arakawa and A. Gomyo, *Appl. Phys. Lett.*, 2007, **91**, 2111041–2111043.
11 P. N. Bartlett, J. J. Baumberg, P. R. Birkin, M. A. Ghanem and M. C. Netti, *Chem. Mater.*, 2002, **14**, 2199–2208.
12 E. Yablonovitch, *Sci. Am.*, 2001, **285**, 46–54.
13 R. Biswas, M. M. Sigalas, G. Subramania, C. M. Soukoulis and K. M. Ho, *Phys. Rev. B: Condens. Matter*, 2000, **61**, 4549–4553.
14 D. Shir, E. C. Nelson, Y. C. Chen, A. Brzezinski, H. Liao, P. V. Braun, P. Wiltzius, K. H. A. Bogart and J. A. Rogers, *Appl. Phys. Lett.*, 2009, **94**, 0111011–0111013.
15 Y. C. Chen, J. B. Geddes, J. T. Lee, P. V. Braun and P. Wiltzius, *Appl. Phys. Lett.*, 2007, **91**, 2411031–2411033.
16 A. Stein, F. Li and N. R. Denny, *Chem. Mater.*, 2008, **20**, 649–666.
17 S. Wong, V. Kitaev and G. A. Ozin, *J. Am. Chem. Soc.*, 2003, **125**, 15589–15598.
18 H. W. Yang, C. F. Blanford, J. C. Lytle, C. B. Carter, W. H. Smyrl and A. Stein, *Chem. Mater.*, 2001, **13**, 4314–4321.
19 Y. A. Vlasov, X. Z. Bo, J. C. Sturm and D. J. Norris, *Nature*, 2001, **414**, 289–293.
20 A. Blanco, E. Chomski, S. Grabtchak, M. Ibisate, S. John, S. W. Leonard, C. Lopez, F. Meseguer, H. Miguez, J. P. Mondia, G. A. Ozin, O. Toader and H. M. van Driel, *Nature*, 2000, **405**, 437–440.
21 J. P. Nicholson, *J. Electrochem. Soc.*, 2005, **152**, C795–C802.
22 Y. Nishimura and Y. Fukunaka, *Electrochim. Acta*, 2007, **53**, 111–116.
23 T. Munisamy and A. J. Bard, *Electrochim. Acta*, 2010, **55**, 3797–3803.
24 N. Borisenko, S. Z. El Abedin and F. Endres, *J. Phys. Chem. B*, 2006, **110**, 6250–6256.
25 S. Z. El Abedin, N. Borissenko and F. Endres, *Electrochem. Commun.*, 2004, **6**, 510–514.
26 X. D. Meng, R. Al-Salman, J. P. Zhao, N. Borissenko, Y. Li and F. Endres, *Angew. Chem., Int. Ed.*, 2009, **48**, 2703–2707.
27 F. Endres, M. Al Zoubi, R. Al-Salman and Y. Li, *Z. Phys. Chem.*, 2011, **225**, 393–403.
28 R. Al-Salman, X. D. Meng, J. P. Zhao, Y. Li, U. Kynast, M. M. Lezhnina and F. Endres, *Pure Appl. Chem.*, 2010, **82**, 1673–1689.
29 J. P. Zhao, Y. Li, Z. Cao and W. H. Xin, *New J. Chem.*, 2008, **32**, 1014–1019.
30 Y. Nishimura, Y. Fukunaka, T. Nishida, T. Nohira and R. Hagiwara, *Electrochem. Solid-State Lett.*, 2008, **11**, D75–D79.
31 J. Stumpe, L. M. Goldenberg, J. Wagner, B. R. Paulke and E. Gornitz, *Langmuir*, 2002, **18**, 3319–3323.